

MARS: CRUSTAL PORE VOLUME, CRYOSPHERIC DEPTH, AND THE GLOBAL OCCURRENCE OF GROUNDWATER; Stephen M. Clifford, Lunar and Planetary Institute, 3303 NASA Rd. 1, Houston, TX, 77058.

There is considerable photogeologic evidence which indicates that Mars, like the Moon, underwent an early period of intense bombardment, producing a "megaregolith" of crater ejecta, interbedded volcanics, weathering products, sediments, and intensely fractured basement, that is likely to extend to considerable depth (1,2). Evidence in support of this conclusion comes from the seismic propagation characteristics of the outer layer of the lunar crust, where P wave velocities increase with depth until they reach a local maximum at about 20 km (3,4,5). This behavior is consistent with a reduction in crustal porosity with increasing lithostatic pressure. The transition between fractured and coherent lunar basement is believed to coincide with the beginning of the constant velocity zone at a depth of 20 km, where lithostatic pressure is thought to be sufficient (>1 kbar) to completely close all fracture and intergranular pore space (3,4,5).

Binder and Lange (5) argue that the seismic properties of the lunar crust are best explained by an exponential decline in porosity with depth (to less than 1% at 20 km). Thus, at a depth z , the porosity is given by

$$\phi(z) = \phi(0) \exp(-z/K) \quad (1)$$

where $\phi(0)$ is the porosity of the crust at $z=0$ and K is the porosity decay constant. Given that the density of the martian crust is comparable to its lunar counterpart, the inferred value of the lunar porosity decay constant (6.5 km) can be gravitationally scaled to find the value appropriate for Mars (2.82 km) (5,6,7).

Applying Eq. (1) to Mars, two potential porosity profiles of the crust are illustrated in Figure 1. The first is based on a surface porosity of 20%, the same value assumed for the Moon by Binder and Lange (5). This model yields a self-compaction depth (the depth at which crustal porosity falls below 1%) of approximately 8.5 km, and a total pore volume of roughly 7.8×10^7 km³. This pore volume is sufficient to store a global layer of water approximately 0.54 km deep. In the second profile, a surface porosity of 50% is assumed, a value that may be appropriate given a significant degree of weathering. The self-compaction depth predicted by this model is roughly 11 km, while its total pore volume is approximately 2×10^8 km³, a volume equivalent to a global ocean some 1.4 km deep. Of course, it is doubtful that weathering will affect more than the upper 1-2 km of the martian crust; therefore, below this depth, the porosity profile will most likely resemble the gravitationally scaled lunar curve.

The fraction of the total pore volume of the martian crust that exists at a temperature below freezing, places an upper limit on the amount of H₂O that can be stored within the crust as ice. This "ground ice capacity" is easily calculated by combining the porosity profiles discussed above with a simple thermal model of the crust (7).

The martian cryosphere has been defined as that region of the crust where the temperature is below the freezing point of water (8). Assuming a solute-free freezing point of 273 K, this condition is satisfied everywhere at the martian surface, thus defining the cryosphere's upper bound. The depth to the cryosphere's lower bound can be calculated from the steady-state one-dimensional heat conduction equation:

$$d = k (T_{mp} - T_{ms})/Q_g \quad (2)$$

where k is the thermal conductivity of the crust, T_{ms} is the mean annual surface temperature, T_{mp} is the melting point temperature, and Q_g is the geothermal heat flux (1,8). Based on a melting point temperature of 273 K, and reasonable estimates of thermal conductivity ($8 \times 10^4 \text{ erg cm}^{-1} \text{ s}^{-1}$) and geothermal heat ($30 \text{ erg cm}^{-2} \text{ s}^{-1}$), the depth to the melting isotherm will vary from approximately 1 km at the equator to slightly in excess of 3 km at the poles (Table 1) (1,8). Of course, given the presence of salt in the regolith, the possibility exists that the freezing point of H_2O could be depressed well below 273 K (9,10). For example, saturated solutions of NaCl and CaCl_2 have associated freezing points of 252 K and 218 K respectively (10). Clearly, the presence of such potent freezing point depressors could reduce the depth to the melting isotherm significantly (Table 1).

Estimates of the total pore volume of the cryosphere can be obtained by integrating the porosity profiles in Figure 1 down to the melting isotherm depths presented in Table 1 for all latitudes. For the variety of possible permutations, the total pore volume of the cryosphere is found to lie within the range of $1.0 \times 10^7 - 9.6 \times 10^7 \text{ km}^3$; while the quantity of H_2O required to saturate this pore volume is equivalent to a global layer of water approximately 70 - 670 meters deep (Table 2).

Given a quantity of H_2O sufficient to fill the available pore volume of the cryosphere, how much additional H_2O is required to produce an aquifer of global proportions? Groundwater will drain to saturate the region of lowest gravitational potential; therefore, the volume of water required to produce an aquifer of a given thickness is calculated by integrating the pore volume of the region between the self-compaction depth and the water table. For example, a quantity of water equivalent to a global layer 10 meters deep is sufficient to saturate the lowermost 0.85 km of the porosity profiles seen in Figure 1; while a quantity of water equal to a 100 meter layer would create an aquifer nearly 4.3 km deep (Figure 2). These figures assume that Mars is a perfect sphere whose porosity profile is everywhere described by Eq. (1). In reality, the self-compaction depth undoubtedly exhibits a high degree of variability. Therefore, because groundwater will collect in the lowermost porous regions of the crust, the actual areal coverage of an aquifer may be substantially less than 100%.

The above calculations suggest that if the planetary inventory of outgassed H_2O on Mars exceeds by more than a few percent the quantity required to saturate the pore volume of the cryosphere, then a subpermafrost groundwater system of substantial proportions will necessarily result (7). This condition may be satisfied by an H_2O inventory as small as 100 m, however, in no event does it appear that it would require more than 700 m. The presences of such a system may have a significant impact on the long-term cycling of H_2O on Mars (7).

REFERENCES:

- 1) Fanale, F. P. (1976) *Icarus* 28, 179-202.
- 2) Carr, M. H. (1979) *J. Geophys. Res.* 84, 2995-3007.
- 3) Toksoz, M. N. (1979) *Rev. Geophys. Space Phys.* 17, 1641-1655.
- 4) Binder, A. B. (1980) *J. Geophys. Res.* 85, 4872-4880.
- 5) Binder, A. B. and M. A. Lange (1980) *J. Geophys. Res.* 85, 3194-3208.
- 6) Clifford, S. M. (1981) *Third Int. Colloq. on Mars*, LPI Cont. 441, 46-48.

MARS: GLOBAL OCCURRENCE OF GROUNDWATER

Clifford, S. M.

- 7) Clifford, S. M. (1984) PhD dissertation, Univ. of Mass., 286 pp.
- 8) Rossbacher, L. A. and S. Judson (1981) Icarus 45, 39-59.
- 9) Brass, G. W. (1980) Icarus 42, 20-28.
- 10) Clark, B. C. and D. C. Van Hart (1981) Icarus 45, 370-378.

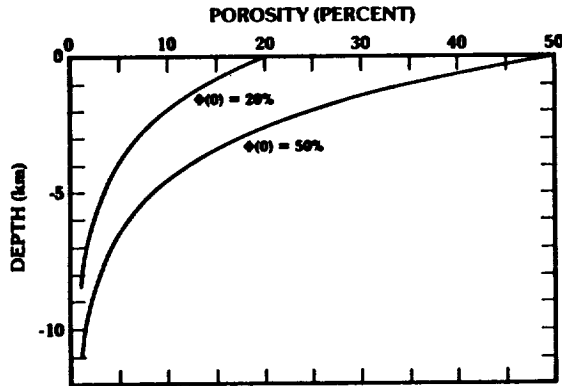


Figure 1

Table 1. Latitudinal variation of cryosphere thickness.*

Latitude	Mean annual surface temperature (K)	Cryosphere depths (km)		
		$T_{mp} = 273$ K	252 K	218 K
0°	225	1.28	0.72	0.0
10°N/S	222	1.36	0.80	0.0
20°N/S	218	1.47	0.91	0.0
30°N/S	215	1.55	0.97	0.08
40°N/S	205	1.81	1.25	0.35
50°N/S	185	2.35	1.79	0.88
60°N	170	2.75	2.19	1.28
60°S	173	2.67	2.11	1.2
70°N	155	3.15	2.59	1.68
70°S	170	2.75	2.19	1.28
80°N	146	3.39	2.83	1.92
80°S	163	2.93	2.37	1.47
90°N	142	3.49	2.93	2.03
90°S	160	3.01	2.45	1.55

*After Ferale (1976) and Rossbacher and Judson (1981).

Table 2. Pore volumes of cryosphere for various surface porosities and melting isotherms temperatures.

Melting Isotherm (K)	Pore volume ($\times 10^7$ km ³)		Equivalent layer of H ₂ O (m)	
	$\phi(0)=20\%$	$\phi(0)=50\%$	$\phi(0)=20\%$	$\phi(0)=50\%$
218	1.01	2.53	70	175
252	2.90	7.26	200	500
273	3.86	9.64	270	670

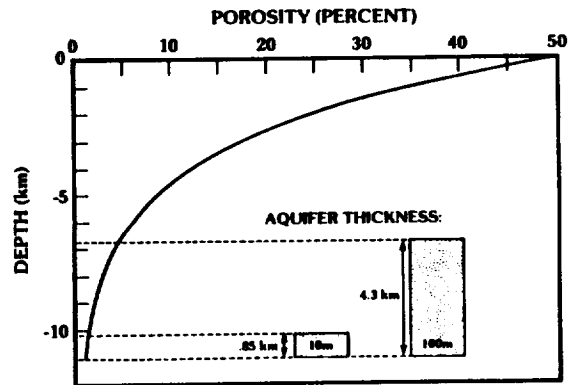


Figure 2